

PCA R&D Serial No. 0878

# Summary of Calibrated Hot Box Test Results for Twenty-One Wall Assemblies

by M. G. Van Geem

# SUMMARY OF CALIBRATED HOT BOX TEST RESULTS FOR TWENTY-ONE WALL ASSEMBLIES

**M.G. Van Geem**

*ASHRAE Member*

## ABSTRACT

Alternative wall systems are frequently evaluated by comparing steady-state heat transmission coefficients, such as U- and R-values. Steady-state transmission coefficients do not adequately describe thermal performance under dynamic temperature conditions. Laboratory results of building envelope components tested under steady-state and dynamic temperature conditions can be used to develop methods of more accurately predicting heat losses and gains to the building envelope.

The thermal characteristics of 21 wall assemblies, including different types of masonry and wood-frame walls and two standard calibration assemblies, have been measured using a calibrated hot box in general accordance with ASTM C976. Results presenting steady-state, transient, and periodic performance have been assembled in two manuals.

This paper summarizes the results. Steady-state values are used to obtain average heat transmission coefficients such as U- and R-values, and the measured values are compared to those calculated from material properties. The transient and periodic dynamic tests provide data on thermal performance under controlled conditions that simulate actual temperature changes in building envelopes. Measured results are compared to values predicted by steady-state analysis. The difference between measured and predicted results is shown to be due in general to thermal storage capacity of the assembly.

## INTRODUCTION

Laboratory results of building envelope components tested under steady-state and dynamic conditions are used to develop methods of accurately predicting losses and gains through the building envelope. Publishing test data in a consistent format will aid researchers in developing dynamic analysis algorithms. Accurately predicting energy consumption will allow architects and engineers to size HVAC equipment optimally and select alternative wall systems on the basis of actual rather than steady-state performance.

The ASHRAE Handbook - 1981 Fundamentals<sup>(1)</sup> summarizes steady-state properties of five commonly used types of wall construction. Thermal and physical properties of building materials used in wall construction are also listed.

A document is needed that summarizes data from tests on wall assemblies under dynamic temperature conditions. Massive materials, such as concrete and masonry, store and release heat energy under changing temperature conditions. Only dynamic tests can be used to determine heat storage characteristics of building components.

This paper summarizes results of tests of 21 wall assemblies, tested under steady-state and dynamic temperature conditions in a calibrated hot box facility. The calibrated hot box pro-

Martha G. Van Geem, Senior Research Engineer, Fire Research Section, Construction Technology Laboratories, a Division of the Portland Cement Association, Skokie, IL 60077.

THIS PREPRINT IS FOR DISCUSSION PURPOSES ONLY. FOR INCLUSION IN ASHRAE TRANSACTIONS 1986, V. 92, Pt. 2. Not to be reprinted in whole or in part without written permission of the American Society of Heating, Refrigerating and Air-Conditioning Engineers, Inc., 1791 Tullie Circle, NE, Atlanta, GA 30329. Opinions, findings, conclusions, or recommendations expressed in this paper are those of the author(s) and do not necessarily reflect the views of ASHRAE.

0878

vides data on heat transmission characteristics of full-size wall assemblies under steady-state and dynamic temperature conditions.

Test data for the 21 wall assemblies are presented in two volumes of a "Calibrated Hot Box Test Results Data Manual."<sup>(2,3)</sup> Heat transfer characteristics of different wall assemblies can be easily compared using figures and summary tables presented for each wall in the manuals. Data presented in numerical form can be used to validate models or analyze results.

Steady-state tests are used to obtain average heat transmission coefficients. The time required for a wall to reach a steady-state condition can be determined from transient tests. Periodic dynamic tests provide data on thermal performance under controlled conditions that simulate actual temperature changes in building envelopes. Dynamic test data are applicable only for the temperature cycles used during testing. Temperature cycles used for tests summarized in this paper cover a variety of temperature conditions. Test results illustrate the significance of dynamic testing.

### TEST SPECIMENS

Table 1 lists descriptions, unit weights, and thicknesses of walls tested in the calibrated hot box. All walls have nominal dimensions of 103 x 103 in (2.62 x 2.62 m). The manuals show an isometric sketch of each wall assembly and list properties, when available, of materials used to construct wall assemblies.

### CALIBRATED HOT BOX TEST FACILITY

Walls were tested in the calibrated hot box facility shown in Figures 1 and 2. Tests were performed generally in accordance with ASTM C976, "Thermal Performance of Building Assemblies by Means of a Calibrated Hot Box."<sup>(4)</sup> Minor differences between test procedures and the ASTM Standard are described in the data manuals.<sup>(2,3)</sup>

The facility consists of two highly insulated chambers as shown in Figure 2. Walls, ceilings, and floors of each chamber are insulated with foamed urethane sheets to obtain a nominal thickness of 12 in (300 mm). During tests, the chambers are clamped tightly against an insulated frame that surrounds the test wall. Air in each chamber is conditioned by heating and cooling equipment to obtain desired temperatures on each side of the test wall.

The outdoor (climatic) chamber can be held at a constant temperature or cycled within the range of -15 to 130F (-26 to 54°C). The outdoor chamber air temperature controller can be programmed to produce the desired time-dependent temperature. The indoor (metering) chamber, which simulates an indoor environment, can be maintained at a constant room temperature between 65F and 80F (18°C and 27°C).

The facility was designed to accommodate walls with thermal resistance values ranging from 1.5 to 20 h·ft<sup>2</sup>·F/Btu (0.26 to 3.52 m<sup>2</sup>·K/W).

Calibration and analysis are briefly described in the following paragraphs. Instrumentation and calibration details are described in References 2, 3, and 5.

Heat flow through a test specimen is determined from measurements of the amount of energy input to the indoor chamber to maintain a constant temperature. The measured energy input must be adjusted for heat losses. Since net energy into the indoor chamber equals zero, heat transfer through the test wall can be expressed by the following energy balance equation.

$$Q_w = Q_c - Q_h - Q_{fan} - Q_l - Q_f \quad (1)$$

where

$Q_w$  = heat transfer through wall from outdoor chamber to indoor chamber

$Q_c$  = heat removed by indoor chamber cooling

$Q_h$  = heat supplied by indoor electrical resistance heaters

$Q_{fan}$  = heat supplied by indoor circulation fan

$Q_l$  = heat gain (loss) from laboratory

$Q_f$  = heat gain (loss) to indoor chamber from flanking path around specimen

Units for terms of Equation 1 are Btu/h (W·h/h).

A watt-hour transducer is used to measure  $Q_h$  and  $Q_{fan}$ . The value of  $Q_l$  is calculated from measured laboratory and indoor chamber temperatures. Heat flux transducers are used to check calculations of  $Q_l$ . Heat removed by indoor chamber cooling,  $Q_c$ , is calculated from refrigerant enthalpy and mass flow rate, assuming an ideal basic vapor compression refrigeration cycle. Steady-state calibrated hot box tests of two "standard" calibration specimens were used to adjust for inefficiencies in the actual refrigeration cycle and to determine  $Q_f$ . In addition to flanking losses, other miscellaneous losses from the indoor chamber are included in  $Q_f$ .

Results from a round robin organized under ASTM Subcommittee C16.30 will provide information on the precision of the calibrated hot box test method.

### THERMAL RESISTANCE

Steady-state calibrated hot box tests were used to measure thermal resistance of wall assemblies. Steady-state tests were conducted by maintaining indoor and outdoor chamber air temperatures constant. Results were calculated from data collected when specimen temperatures reached equilibrium and the rate of heat flow through the wall was constant.

Measured and design thermal resistances are listed in Table 2. Mean wall temperatures for each steady-state test are also indicated.

Measured total thermal resistance,  $R_T$ , is the sum of measured wall resistance and design air film resistances. Wall resistance was determined from measured heat flux and surface-to-surface temperature differentials. Air film resistances were taken as  $0.68 \text{ h}\cdot\text{ft}^2\cdot\text{F}/\text{Btu}$  ( $0.12 \text{ m}^2\cdot\text{K}/\text{W}$ ) for inside and  $0.17 \text{ h}\cdot\text{ft}^2\cdot\text{F}/\text{Btu}$  ( $0.03 \text{ m}^2\cdot\text{K}/\text{W}$ ) for outside. These values are commonly used in design and are considered to represent still air on the indoor wall surface and an airflow of 15 mph (24 km/h) on the outdoor wall surface.<sup>(1)</sup>

Design values of total resistance were calculated using standard surface resistances in accordance with procedures established by ASHRAE.<sup>(1)</sup> The parallel-path method was used to include the effect of framing in calculated R-values of frame wall systems. Resistances for construction materials were taken from the ASHRAE Handbook - 1981 Fundamentals<sup>(1)</sup> or other similar listings of thermal properties. The data manuals<sup>(2,3)</sup> indicate sources for construction material resistances. Resistances of individual wall components used to calculate design values were not measured.

### DYNAMIC TEST RESULTS

Periodic dynamic tests are a means of evaluating thermal response under controlled conditions that simulate temperature changes actually encountered in building envelopes. The response of walls to temperature changes is a function of both thermal resistance and heat storage capacity. Overall resistance includes wall resistance and surface resistance characteristics.

#### Test Procedures

Dynamic tests were conducted by maintaining calibrated hot box indoor air temperature constant while outdoor air temperatures were cycled over a predetermined temperature versus time relationship. The rate of heat flow through a test specimen was determined from hourly averages of data.

One 24-hour (diurnal) temperature cycle, denoted the NBS Test Cycle, was applied to every wall tested in the calibrated hot box. This cycle was based on a simulated sol-air\* cycle used by the National Bureau of Standards in their evaluation of dynamic thermal performance of an experimental masonry building.<sup>(6)</sup> The NBS Cycle, illustrated in Figure 3, represents a large variation in outdoor temperature over a 24-hour period. The mean outdoor temperature of the cycle is approximately equal to the mean indoor temperature. The indoor chamber temperature is maintained at approximately 72F (22°C). The use of this cycle permits the comparison of results for all tested wall assemblies.

Additional sol-air diurnal temperature cycles were performed on most test specimens. Test results and descriptions of these cycles are available in the data manuals.<sup>(2,3)</sup>

For all tests, dynamic cycles were repeated until conditions of "dynamic equilibrium" were obtained. Equilibrium conditions were evaluated by repeatability of applied temperatures and measured heat flux. After equilibrium conditions were reached, tests were generally continued for a period of three days. Results are based on average readings for three consecutive 24-hour cycles, unless otherwise noted. Each test required approximately four to six days for completion.

### Data Presentation

The data manuals<sup>(2,3)</sup> present heat flux values for every dynamic cycle applied to each wall assembly. Data are presented in tabular form and in figures.

Figure 4(a) shows measured and calculated heat flux for the NBS Test Cycle applied to Wall C1. Heat flux is positive when heat flows from the outdoor chamber to the indoor chamber. Heat flux at the inside surface of the wall, measured by the calibrated hot box, is denoted  $q_w$ . Measurements from 4 x 4-in (100 x 100-mm) heat flux transducers located on indoor and outdoor wall surfaces are denoted  $q_{hfm}$  and  $q'_{hfm}$ , respectively. Heat flux transducer data were calibrated using results of steady-state calibrated hot box tests for the specimen.

Heat flux predicted by steady-state analysis is denoted  $q_{ss}$ . Values were calculated on an hourly basis from wall surface temperatures using the following equation:

$$q_{ss} = (t_2 - t_1) / R \quad (2)$$

### where

$q_{ss}$  = heat flux through test wall predicted by steady-state analysis, Btu/h·ft<sup>2</sup> (W/m<sup>2</sup>)

$R$  = measured thermal resistance, h·ft<sup>2</sup>·F/Btu (m<sup>2</sup>·K/W)

$t_2$  = average temperature of outdoor wall surface

$t_1$  = average temperature of indoor wall surface

Resistances are dependent on wall mean temperature and are derived from steady-state calibrated hot box tests. Measured thermal resistance,  $R$ , is equal to the total resistance,  $R_T$ , listed in Table 2, minus the sum of the design air film resistances, 0.85 h·ft<sup>2</sup>·F/Btu (0.15 m<sup>2</sup>·K/W).

Data manual tables list hourly values of calculated and measured heat flux. Tables also footnote the calibrated hot box indoor and outdoor chamber relative humidities and maximum and minimum laboratory air temperatures measured during tests.

### Dynamic Heat Transmission Coefficients

Thermal lag, reduction in amplitude, and the total heat flow ratio are three coefficients used to describe test specimen behavior under dynamic temperature conditions. These coeffi-

\*Sol-air temperature is that temperature of outdoor air that, in the absence of all radiation exchanges, would give the same rate of heat entry into the surface as would exist with the actual combination of incident solar radiation, radiant energy exchange, and convective heat exchange with outdoor air.<sup>(1)</sup>

cients characterize thermal storage capacity and are derived from comparisons of measured results to values predicted on the basis of steady-state analysis.

Thermal Lag and Reduction in Amplitude. Thermal lag and reduction in amplitude are used to describe wall dynamic thermal performance for a particular dynamic temperature cycle. Thermal lag, as illustrated in Figure 4(b), is the difference in time between peak values of measured heat flow,  $q_w$ , and heat flow based on steady-state predictions,  $q_{SS}$ . Thermal lag is of interest because the time of occurrence of peak heat flows will have an effect on overall response of the building envelope. If the envelope can be effectively used to delay the occurrence of peak loads, it may be possible to improve overall energy efficiency. The "lag effect" is also useful for passive solar applications.

Reduction in amplitude, also illustrated in Figure 4(b), is the percent reduction in actual peak heat flux when compared to peak heat flux calculated using steady-state theory. Actual maximum heat flux through a wall is important in determining the peak energy load for a building envelope. Using actual peak heat flow rather than heat flow based on steady-state theory may reduce anticipated energy demands. Reduction in amplitude is calculated using the following equation:

$$A = [1 - (q'_w - \bar{q}_w) / (q'_{SS} - \bar{q}_{SS})] \cdot 100 \quad (3)$$

A = reduction in amplitude, %

$q'_w$  = maximum or minimum measured heat flux through wall

$\bar{q}_w$  = mean measured heat flux through wall

$q'_{SS}$  = maximum or minimum heat flux through wall predicted by steady-state analysis

$\bar{q}_{SS}$  = mean heat flux through wall predicted by steady-state analysis

Average reduction in amplitude is the average of values determined for maximum and minimum heat flux.

The data manuals(2,3) contain summary tables that present thermal lag and reduction in amplitude for each dynamic temperature cycle applied to a wall assembly.

Total Heat Flow Ratio. Results of dynamic tests are compared also using measures of total heat flux through a test specimen, illustrated in Figure 4(b). The curve marked " $q_w$ " is measured heat flux through the test wall. Shaded areas enclosed by the measured heat flux curves and the horizontal axis are used to determine total measured heat flux. The sum of the areas above and below the horizontal axis is the total heat flux over a 24-hour period.

A similar procedure is used to calculate total heat flux over a 24-hour period for predictions based on steady-state analysis. The total heat flow ratio is the ratio of total measured heat flux to total predicted heat flux based on steady-state analysis. The ratio is represented as a percentage.

The data manuals(2,3) contain summary tables that present total measured heat flux, total heat flux based on steady-state analysis, and the total heat flow ratio. Values are presented for each dynamic temperature cycle applied to a wall assembly.

### Comparing Wall Systems

Dynamic heat transmission coefficients are used to compare dynamic thermal response of alternative wall systems.

Thermal lag and reduction in amplitude are dependent on both thermal resistance, R, and heat storage capacity,

$\rho c L$

where

$\rho$  = wall density, pcf (kg/m<sup>3</sup>)

c = wall specific heat, Btu/lb·F (J/kg·K)

L = wall thickness, ft (m)

Mass,  $\rho L$ , is the predominant factor in determining heat storage capacity of most building materials.

For homogeneous walls, thermal lag and reduction in amplitude increase with an increase in  $M$  (12)

$$M = \left( \frac{L^2/\alpha}{P} \right)^{1/2} = \left( \frac{(R) \cdot (\rho c L)}{P} \right)^{1/2} \quad (4)$$

where

L = wall thickness, ft (m)

$\alpha$  = thermal diffusivity,  $k/\rho c$ , ft<sup>2</sup>/h (m<sup>2</sup>/s)

k = thermal conductivity of wall, Btu/h·ft·F (W/m·K)

$\rho$  = wall density, pcf (kg/m<sup>3</sup>)

c = wall specific heat, Btu/lb·F (J/kg·K)

R = wall resistance, h·ft<sup>2</sup>·F/Btu (m<sup>2</sup>·K/W)

P = period of dynamic cycle, h

Values of M were calculated for the 21 walls listed in Volumes 1 and 2 of the data manuals. Thermal resistances used in Equation 4 were either measured, or obtained from the ASHRAE Handbook - 1981 Fundamentals(1) or other similar listings. Surface resistances are not included in resistances used in Equation 4.

Unit weights of masonry materials were determined from measured oven-dry material unit weights and estimated moisture contents. Other unit weights were either measured or estimated using properties listed in Reference 1. Values of specific heat were determined from References 1 and 13. Equivalent thicknesses for block and brick are equal to the product of the layer width and percent solid volume. Values of M for individual wall layers are summed to determine total wall M values.

Thermal Lag. Lag times of 9 to 15 hours are generally beneficial for exterior walls. Walls with these lag times delay peak afternoon heat loads until cooler night hours. Thermal lags as low as 3 hours are beneficial in delaying peak afternoon loads until cooler evening hours. These lower lag times are especially beneficial in commercial and industrial buildings that are vacated in the evening hours.

Figure 5 shows measured thermal lag versus calculated M for 21 wall assemblies. Measured thermal lags are for the NBS temperature cycle applied to each wall assembly. Thermal lag is constant for any given wall assembly, regardless of the temperature cycle applied.

Measured thermal lag increases with values of M. Walls S1 and S2, consisting of insulation only, have smallest lag times. Wall S2 has a larger lag and M value than Wall S1 because of its greater thickness and thermal resistance. Walls F1, F3, F4, and F5, insulated frame walls, have greater thermal lags and M values than Walls S1 and S2 because of the increase in mass of the 2 x 4-in (50 x 100-mm) wood frames.

Walls M1 and M5, uninsulated concrete block, have the next highest thermal lags, equal to 3 hours. Walls with thermal lags from 3.5 to 4.5 hours include Walls M2, M6, M7, and M8, insulated concrete block; Wall V1, brick veneer; and Wall C1, normal weight concrete. Walls M3 and M9, the uninsulated block-brick cavity walls, have thermal lags of 4.5 and 5.5 hours, respectively. Wall C4, normal weight concrete with insulation, and Wall C2, structural lightweight concrete have relatively large thermal lags, equal to 5 and 5.5 hours, respectively. Walls M4 and M10, the insulated cavity walls, have thermal lags of 6 and 7 hours, respectively.

Wall C3, low density concrete, has the greatest lag time, equal to 8.5 hours. Concrete in Wall C3 has mass as well as a higher resistance than most concrete and masonry materials. Equation 4 shows that thermal lag and M are dependent on both mass and resistance.

Four walls were constructed by adding insulation to masonry or concrete walls previously tested in the hot box. Table 3 shows thermal lags were increased 0.5 to 1.5 hours when insulation was added. These increases in thermal lags due to the addition of insulation may be predicted by the increase in M from Equation 4.

Wall V1 was constructed by adding a brick veneer to Wall F3, an insulated frame wall. Addition of the brick veneer increased thermal lag 1.5 hours, from 2.5 to 4 hours.

Reduction in Amplitude. Figure 6 shows average measured reduction in amplitude versus calculated M for 19 wall assemblies. Since reduction in amplitude values vary depending on the temperature cycle applied to a given wall assembly, values presented in Figure 6 were determined from the NBS test cycle applied to each wall assembly.

Figure 6 shows that concrete and masonry walls, designated C and M, respectively, generally have greater reduction in amplitude than insulation and insulated frame walls, designated S and F, respectively. This is due to the storage capacity or mass of the concrete and masonry walls.

More scatter exists for data points in Figure 6 than for Figure 5. This indicates M predicts thermal lag better than reduction in amplitude. Wall C4, concrete with insulation on the outdoor surface, has a higher reduction in amplitude than other wall assemblies with similar M values. The parameter M does not include placement of insulation with respect to thermal mass.

Total Heat Flow Ratio. Figure 7 shows measured total heat flow ratio versus calculated M for 19 wall assemblies. The heat flow ratio is the total heat flow for a 24-hour period measured by the calibrated hot box,  $q_w^T$ , divided by total heat flow for the same period predicted using steady-state analysis,  $q_{ss}^T$ . Since total heat flow ratios vary depending on the temperature cycle applied to a given wall assembly, values in Figure 7 are for the NBS test cycle applied to each wall assembly.

Figure 7 shows that concrete and masonry walls, designated C and M, respectively, generally have lower total heat flow ratios than insulation or insulated frame walls, designated S and F, respectively. The lower total heat flow ratios are due to the storage capacity of the masonry. Figure 7 also shows that the total heat flow ratio for Wall C4, concrete with insulation on the outdoor surface, is lower than for other walls with similar M values.

It should be noted that comparison of measured heat flux values for the test walls is limited to specimens and dynamic cycles evaluated in this program. Results are for diurnal test cycles and should not be arbitrarily assumed to represent annual heating and cooling loads. In addition, results are for individual opaque wall assemblies. As such, they are representative of only one component of the building envelope.

## TRANSIENT TEST RESULTS

Time required for a wall to reach a steady-state condition can be determined from transient tests. This time is affected by both thermal resistance and heat storage capacity of the test wall.

### Test Procedures

Results of a transient test are determined from data collected in the period of time between two steady-state tests. After a wall is in a steady-state condition, the outdoor chamber temperature setting is changed. The transient test continues until the wall reaches an equilibrium for the new outdoor chamber air temperature. Measured heat flux and temperatures are summarized hourly during transient tests.

Transient tests were performed for Walls M9, M10, C1, C2, C3, C4, and F1. Initial outdoor and indoor chamber air temperatures were  $72.5 \pm 1F$  ( $22.5 \pm 0.6^\circ C$ ) and  $72.3 \pm 0.4F$  ( $22.4 \pm 0.2^\circ C$ ), res-



pectively. Final outdoor and indoor chamber air temperatures were  $-8 \pm 6F$  ( $-22 \pm 3^\circ C$ ) and  $70.5 \pm 2F$  ( $21.4 \pm 1^\circ C$ ), respectively.

The data manuals(2,3) present transient test results in figures and tables. Figures show measured air temperatures, measured wall temperatures, heat flux measured by the calibrated hot box, heat flux measured by heat flux transducers, and heat flux predicted by steady-state analysis. Tables list hourly values of data shown in figures. A summary table of transient test results lists time required to reach 90%, 95%, and 99.5% of the final, steady-state heat flux achieved during a transient test.

### Comparing Wall Systems

If the difference in temperature across a wall is changed abruptly from the steady-state condition, as in a step change, then the heat flow through the wall will theoretically equal 63.2% of the next steady-state equilibrium heat flow after a time period equal to the time constant.(14) A time constant is a theoretical value of heat flow delay calculated from the conductivity, specific heat, density, and thickness for each layer of building material in a wall system.

The following equation was used to calculate time constants:(14)

$$t_c = \frac{a_k}{\pi} \left( \sum_{n=1}^N (g_n X_n) \right)^2 \quad (5)$$

where

$t_c$  = characteristic time constant of building component, h(s)

$g_n = (a_n/a_k)^{1/2}$ , conversion constant adjusting thickness of layer to make material uniform throughout wall

$a_n = (r_n c_n d_n)$ , reciprocal of diffusivity of n-th layer, h/ft<sup>2</sup> (s/m<sup>2</sup>)

$a_k = a_n$  at layer k chosen for normalization

$r_n$  = resistivity of n-th layer, or reciprocal of conductivity of n-th layer h·ft·F/Btu (m·K/W)

$c_n$  = specific heat of n-th layer, Btu/lb·F (J/kg·K)

$d_n$  = density of n-th layer, lb/ft<sup>3</sup> (kg/m<sup>3</sup>)

$X_n$  = thickness of n-th layer, ft (m)

When available, measured thermal properties for each wall assembly were used to calculate time constants. Properties from the ASHRAE Handbook - 1981 Fundamentals(1) were used when measured values were not available.

Figure 8 shows calculated time constants and calibrated hot box transient test results. The vertical axis is time required to reach 63.2% of the final heat flux measured by the calibrated hot box, designated  $t_c'$ . The calibrated hot box cannot simulate the same step-change in temperature assumed in the definition of a time constant. Cooling system equipment limitations and storage capacity of the outdoor chamber prohibit an ideal step-change. Many hours elapse before the outdoor chamber air reaches an equilibrium temperature.

Measured  $t_c'$  values increase with increasing values of calculated  $t_c$ . Wall F1, the insulated wood frame wall, has lower measured  $t_c'$  and calculated  $t_c$  than the masonry walls. Adding insulation to the cavity of Wall M9, a block-brick cavity wall, to form Wall M10, increased both measured  $t_c'$  and calculated  $t_c$ .

Adding insulation to the outdoor surface of Wall C1, normal weight concrete, to form Wall C4, increased the measured  $t_c'$  80%, from 10 to 18 hours. This compares to a calculated time constant for Wall C4 10% greater than Wall C1.

## SUMMARY AND CONCLUSION

This paper summarizes measured thermal characteristics of 21 wall assemblies presented in Volumes I and II of the "Calibrated Hot Box Test Results Data Manual."<sup>(2,3)</sup> Results are presented for six concrete masonry (block) walls, four masonry (block-brick) cavity walls, three concrete walls, a concrete wall with exterior insulation, four wood-frame walls, a brick veneer-wood frame wall, and two standard calibration walls. One standard wall was comprised of 4-in (100-mm) polystyrene beadboard and one was 1 3/8-in (35-mm) fiberglass board. The manuals present steady-state, transient, and dynamic (periodic) test results in tabular form, in figures, and in summary tables. Heat transfer characteristics of different wall assemblies can be compared by using figures and summary tables for each wall. Data presented in numerical form can be used to validate models or to further analyze results.

The following conclusions are based on results obtained in this investigation.

1. Total thermal resistance,  $R_T$ , measured using the calibrated hot box and calculated using handbook values, are presented for 21 wall assemblies.
2. Thermal lag, reduction in amplitude, and the total heat flow ratio are three coefficients used to describe test specimen behavior under dynamic temperature conditions. These coefficients are dependent on resistance and storage capacity of a given wall assembly. Reduction in amplitude and total heat flow ratio are also dependent on the temperature cycle applied to the wall.
3. Concrete and masonry walls have greater thermal lags than insulation and insulated frame walls.
4. Wall C3, constructed of low density concrete, has a lag time equal to 8.5 hours. This is the largest lag time of the 21 wall assemblies summarized in this paper.
5. Adding insulation to concrete and masonry walls increased thermal lags by 0.5 to 1.5 hours. Insulation was added to the outside surface of the concrete wall, to the cores of the block wall, and to the cavity of the masonry cavity walls.
6. Adding a brick veneer to an insulated wood frame wall increased thermal lag 1.5 hours, from 2.5 to 4 hours.
7. Concrete and masonry walls have greater reduction in amplitude than insulation and insulated frame walls for tests using the NBS dynamic temperature cycle.
8. Concrete and masonry walls have lower total heat flow ratios than insulation and insulated frame walls for tests using the NBS dynamic temperature cycle.
9. Transient test results indicate concrete and masonry walls delay heat flow longer than insulation or insulated frame walls. This is due to the thermal storage capacity of the concrete and masonry walls.
10. Transient test results indicate that heat flow is delayed by the addition of an insulation layer to a concrete or masonry wall.

Results described in this paper provide data on thermal response of walls subjected to steady-state and diurnal sol-air temperature cycles. A complete analysis of building energy requirements must include consideration of the entire building envelope, building orientation, building operation, and yearly weather conditions.

Laboratory results of building envelope components tested under steady-state and dynamic conditions are used to develop methods of accurately predicting losses and gains through the building envelope. Publishing test data in a consistent format will aid researchers developing dynamic analysis algorithms. Accurately predicting energy consumption will allow architects and engineers to size HVAC equipment optimally and select alternative wall systems on the basis of actual rather than steady-state performance.

## REFERENCES

1. ASHRAE Handbook - 1981 Fundamentals, American Society of Heating, Refrigeration, and Air-Conditioning Engineers, Inc., Atlanta, Georgia, 1981
2. Van Geem, M. G., "Calibrated Hot Box Test Results Data Manual - Volume I," Construction Technology Laboratories, Portland Cement Association, Skokie, Illinois, 1984, 336 pages.
3. Van Geem, M. G., and Larson, S. C., "Calibrated Hot Box Test Results Data Manual - Volume II," Construction Technology Laboratories, Portland Cement Association, Skokie, Illinois, 1985, 164 pages.
4. 1984 Annual Book of ASTM Standards, American Society for Testing and Materials, Philadelphia, Pennsylvania, 1984.
5. Fiorato, A. E., "Laboratory Tests of Thermal Performance of Exterior Walls," Proceedings of the ASHRAE/DOE-ORNL Conference on Thermal Performance of the Exterior Envelopes of Buildings, Orlando, Florida, Dec. 1979, ASHRAE SP28, Atlanta, Georgia, 1981, pp. 221-236.
6. Peavy, B. A., Powell, F. J., and Burch, D. M., "Dynamic Thermal Performance of an Experimental Masonry Building," Building Science Series 45, U.S. Department of Commerce, National Bureau of Standards, Washington, DC, 1973.
7. Van Geem, M. G., and Larson, S. C., "Heat Transfer Characteristics of a Masonry Cavity Wall with and without Expanded Perlite Insulation," Construction Technology Laboratories, Portland Cement Association, Skokie, Illinois, 1984, 142 pages.
8. Fiorato, A. E., "Heat Transfer Characteristics of Walls Under Dynamic Temperature Conditions," Research and Development Bulletin RD075, Portland Cement Association, Skokie, Illinois, 1981, 20 pages.
9. Fiorato, A. E. and Bravinsky, E., "Heat Transfer Characteristics of Walls Under Arizona Temperature Conditions," Construction Technology Laboratories, Portland Cement Association, Skokie, Illinois, 1981, 61 pages.
10. Larson, S. C., and Van Geem, M. G., "Heat Transfer Characteristics of Walls with Similar Thermal Resistance Values," Construction Technology Laboratories, Portland Cement Association, Skokie, Illinois, 1985, 145 pages.
11. Van Geem, M. G., Fiorato, A. E., and Julien, J. T., "Heat Transfer Characteristics of a Normal Weight Concrete Wall," Construction Technology Laboratories, Portland Cement Association, Skokie, Illinois, 1983, 89 pages.
12. Childs, K. W., Courville, G. E., and Bales, E. L., "Thermal Mass Assessment," Oak Ridge National Laboratory for the U.S. Department of Energy, Oak Ridge, Tennessee, 1983, 86 pages.
13. Van Geem, M. G., and Fiorato, A. E., "Thermal Properties of Masonry Materials for Passive Solar Design - A State-of-the-Art Review," Construction Technology Laboratories, Portland Cement Association, Skokie, Illinois, 1983, 86 pages.
14. Flanders, S. N., "Time Constraints on Measuring Building R-Values," CRREL Report 80-15, United States Army, Corps of Engineers, Cold Regions Research and Engineering Laboratory, Hanover, New Hampshire, 1980, 30 pages.

## ACKNOWLEDGMENTS

This work was performed in the Engineering and Resource Development Division of the Construction Technology Laboratories (CTL), a Division of the Portland Cement Association, under the direction of Dr. W. G. Corley, executive director, and Mr. D. W. Musser, formerly director of the Construction Methods Department. The paper was prepared as part of a project sponsored by the Portland Cement Association.

The data manuals were prepared as part of a project sponsored jointly by the U.S. Department of Energy, Office of Building and Community Systems, and the Portland Cement Association. The work is under subcontract 86X-42539C with Oak Ridge National Laboratory (ORNL), operated by Martin Marietta Energy Systems, Inc., for the U.S. Department of Energy. It is part of the National Program Plan for Building Thermal Envelope Systems and Materials.

Mr. S. C. Larson, associate research engineer, assisted in data reduction and analysis. He also reviewed the manuscript and provided helpful comments and suggestions.

Mrs. E. Ringquist provided editorial assistance in preparation of the manuscript. The manuscript was typed by personnel of the Portland Cement Association's Word Processing Department. Mr. C. Steer drafted the figures.

TABLE 1  
Wall Descriptions

Wall Designation	Wall Description	Measured Unit Weight, psf <sub>2</sub> (kg/m <sup>2</sup> )	Measured Thickness, in (mm)
M1	Medium Weight Hollow Core Concrete Block	40.1 (196)	7.6 (195)
M2	Medium Weight Hollow Core Concrete Block with Loose-Fill Insulation in Cores	40.9 (200)	7.6 (195)
M5	8-in (200-mm) Normal Weight Hollow Core Concrete Block with Stucco on Outside Surface and Foil-Backed Gypsum Wall Board Secured to Furring Strips on Inside Surface	48.2 (235)	9.4 (240)
M6	8-in (200-mm) Lightweight Hollow Core Concrete Block with R-8 Fiberglass Batt Insulation Between Furring Strips and Gypsum Wallboard on Inside Surface	42.1 (205)	9.9 (25)
M7	6-in (150-mm) Lightweight Hollow Core Concrete Block with R-8 Fiberglass Batt Insulation Between Furring Strips and Gypsum Wallboard on Inside Surface	33.4 (163)	7.9 (200)
M8	8-in (200-mm) Normal Weight Hollow Core Concrete Slump Block with R-8 Fiberglass Batt Insulation Between Furring Strips and Gypsum Wallboard on Inside Surface	48.9 (239)	9.4 (240)
M3	Uninsulated Cavity Wall: 4-in (100-mm) Hollow Core Concrete Block and 4-in (100-mm) Clay Brick Separated by a 2-in (50-mm) Air Space	66.7 (326)	9.6 (245)
M4	Insulated Cavity Wall: 4-in (100-mm) Hollow Core Concrete Block and 4-in (100-mm) Clay Brick Separated by 2-in (50-mm) of Loose-Fill Insulation	67.7 (331)	9.6 (245)
M9	Uninsulated Cavity Wall: 6-in (145-mm) Hollow Core Concrete Block and 4-in (85-mm) Clay Brick Separated by a 2.8-in (70-mm) Air Space	81.0 (395)	12.1 (305)
M10	Insulated Cavity Wall: 6-in (145-mm) Hollow Core Concrete Block and 4-in (85-mm) Clay Brick Separated by 2.8-in (70-mm) of Loose-Fill Insulation	82.0 (400)	12.1 (305)
C1	Normal Weight Concrete	100 (488)	8.3 (210)
C2	Structural Lightweight Concrete	70.4 (344)	8.3 (210)
C3	Low Density Concrete	32.7 (160)	8.5 (215)
C4	8-in (200-mm) Normal Weight Concrete with R-5 Insulation Board Applied to Outside Surface	98.5 (480)	8.9 (225)

TABLE 1  
Wall Descriptions (Cont'd)

Wall Designation	Wall Description	Measured Unit Weight, psf <sub>2</sub> (kg/m <sup>2</sup> )	Measured Thickness, in (mm)
F1	2x4-1n (50x100-mm) Wood Frame with R-13 Fiberglass Batt Insulation between Studs, Gypsum Wallboard on Inside Surface, and R-5 Board Insulation and Aluminum Siding on Outside Surface	4.0 (20)	5.6 (140)
F3	2x4-1n (50x100-mm) Wood Frame with R-11 Fiberglass Batt Insulation between Studs, Gypsum Wallboard on Inside Surface, and Plywood Cedar Siding on Outside Surface	5.2 (25)	4.6 (120)
F4	2x4-1n (50x100-mm) Wood Frame with R-11 Fiberglass Batt Insulation between Studs, Gypsum Wallboard on Inside Surface, and Plywood Cedar Siding on Outside Surface	5.3 (26)	4.8 (120)
F5	2x4-1n (50x100-mm) Wood Frame with R-11 Fiberglass Batt Insulation between Studs, Gypsum Wallboard on Inside Surface, and Hardwood Siding on Outside Surface	4.7 (23)	4.3 (110)
V1	Wood Frame Wall F3 with 4-1n (100-mm) Clay Brick Applied 1 in (25 mm) from Cedar Siding	45.1 (220)	9.2 (235)
S1	Fiberglass Board Insulation with Foil Facing Applied to Inside and Outside Surfaces	1.1 (5.2)	1.5 (37)
S2	Polystyrene Beadboard Insulation with Carpet Adhesive Applied to Inside and Outside Surfaces	0.6 (2.7)	4.0 (100)

TABLE 2  
Measured and Design Thermal Resistance

Wall Designation	Wall Description	Measured		Design
		Wall Mean Temperature, F (°C)	Thermal Resistance $R_T^*$ , $\text{h}\cdot\text{ft}^2\cdot\text{F}/\text{Btu}$ ( $\text{m}^2\cdot\text{K}/\text{W}$ )	Thermal Resistance $R_T$ , $\text{h}\cdot\text{ft}^2\cdot\text{F}/\text{Btu}$ ( $\text{m}^2\cdot\text{K}/\text{W}$ )
M1	8-in (200-mm) Medium Weight Concrete Block	55 (13)	2.65 (0.47)	2.37 (0.42)
		84 (29)	2.93 (0.52)	
		--	--	
M2	8-in (200-mm) Medium Weight Concrete Block with Insulation in Cores	33 (1)	4.54 (0.80)	4.85 (0.85)
		98 (37)	4.24 (0.75)	
		--	--	
M5	8-in (200-mm) Normal Weight Concrete Block with Reflective Insulation	35 (2)	5.76 (1.01)	5.33 (0.94)
		100 (38)	5.54 (0.98)	
		--	--	
M6	8-in (200-mm) Lightweight Concrete Block with Insulation on Inside Surface	38 (3)	9.03 (1.59)	8.33 (1.56)
		102 (39)	7.40 (1.39)	
		--	--	
M7	6-in (150-mm) Lightweight Concrete Block with Insulation on Inside Surface	38 (3)	9.08 (1.60)	8.22 (1.45)
		102 (39)	7.90 (1.39)	
		--	--	
M8	8-in (200-mm) Normal Weight Concrete Block with Insulation on Inside Surface	39 (4)	8.03 (1.41)	7.67 (1.35)
		102 (39)	7.12 (1.25)	
		--	--	
M3	10-in (250-mm) Block-Brick Cavity Wall	36 (12)	3.59 (0.63)	3.46 (0.61)
		97 (36)	3.61 (0.64)	
		--	--	
M4	10-in (250-mm) Block-Brick Cavity Wall with Insulation in Cavity	33 (1)	8.33 (1.47)	8.55 (1.51)
		98 (37)	8.54 (1.50)	
		--	--	
M9	12-in (300-mm) Block-Brick Cavity Wall	32 (0)	3.64 (0.64)	3.47 (0.61)
		100 (38)	3.37 (0.59)	
		--	--	
M10	12-in (300-mm) Block-Brick Cavity Wall with Insulation in Cavity	32 (0)	9.32 (1.64)	8.83 (1.56)
		100 (38)	9.47 (1.67)	
		--	--	
C1	8-in (200-mm) Normal Weight Concrete	37 (3)	1.56 (0.28)	1.54 (0.27)
		55 (13)	1.56 (0.28)	
		101 (38)	1.55 (0.27)	
		--	--	

\*Total thermal resistance,  $R_T$ , is the sum of measured wall resistance and design air film resistances of  $0.17 \text{ h}\cdot\text{ft}^2\cdot\text{F}/\text{Btu}$  ( $0.03 \text{ m}^2\cdot\text{K}/\text{W}$ ) for outside and  $0.68 \text{ h}\cdot\text{ft}^2\cdot\text{F}/\text{Btu}$  ( $0.12 \text{ m}^2\cdot\text{K}/\text{W}$ ) for inside. Wall resistance was determined from measured heat flux and surface-to-surface temperature differentials.

TABLE 2  
Measured and Design Thermal Resistance (Cont'd)

Wall Designation	Wall Description	Measured		Design
		Wall Mean Temperature, F (°C)	Thermal Resistance $R_T^*$ , h·ft <sup>2</sup> ·F/Btu (m <sup>2</sup> ·K/W)	Thermal Resistance $R_T^*$ , h·ft <sup>2</sup> ·F/Btu (m <sup>2</sup> ·K/W)
C2	8-in (200-mm) Structural Lightweight Concrete	34 (1)	2.63 (0.46)	3.05 (0.54)
		52 (11)	2.62 (0.46)	
		88 (31)	2.59 (0.46)	
		99 (37)	2.56 (0.45)	
		--	--	
C3	8-in (200-mm) Low Density Concrete	53 (11)	7.02 (1.24)	
		89 (32)	6.53 (1.15)	
		100 (38)	6.31 (1.11)	
		--	8.87 (1.56)	
C4	8-in (200-mm) Normal Weight Concrete with R-5 Insulation Board on Outside Surface	32 (0)	7.85 (1.38)	6.04 (1.06)
		101 (38)	7.57 (1.33)	
		--	--	
F1	2x4-in (50x100-mm) Wood Frame with R-13 Fiberglass Insulation and R-5 Insulation Board	30 (-1)	19.17 (3.38)	19.08 (3.36)
		101 (39)	16.42 (2.89)	
		--	--	
F3	2x4-in (50x100-mm) Wood Frame with R-11 Fiberglass Insulation and Cedar Siding	33 (0)	15.9 (2.63)	11.4 (2.01)
		98 (37)	13.6 (2.39)	
		--	--	
F4	2x4-in (50x100-mm) Wood Frame with R-11 Fiberglass Insulation and Cedar Siding	34 (1)	13.0 (2.29)	11.1 (1.95)
		54 (12)	13.0 (2.28)	
		100 (38)	10.8 (1.90)	
		--	--	
F5	2x4-in (50x100-mm) Wood Frame with R-11 Fiberglass Insulation and Hard-board Siding	38 (3)	12.0 (2.11)	11.0 (1.94)
		102 (39)	10.0 (1.77)	
		--	--	
V1	10-in (250-mm) Brick Veneer	33 (0)	17.0 (2.99)	12.8 (2.25)
		99 (37)	14.3 (2.52)	
		--	--	
S1	1-3/8-in (35-mm) Fiberglass Board	32 (0)	7.10 (1.25)	6.35 (1.12)
		103 (40)	6.50 (1.14)	
		--	--	
S2	4-in (100-mm) Polystyrene Beadboard	37 (3)	19.8 (3.49)	17.5 (3.09)
		53 (12)	17.5 (3.08)	
		101 (38)	16.5 (2.90)	
		--	--	

\*Total thermal resistance,  $R_T$ , is the sum of measured wall resistance and design air film resistances of 0.17 h·ft<sup>2</sup>·F/Btu (0.03 m<sup>2</sup>·K/W) for outside and 0.68 h·ft<sup>2</sup>·F/Btu (0.12 m<sup>2</sup>·K/W) for inside. Wall resistance was determined from measured heat flux and surface-to-surface temperature differentials.



TABLE 3  
Increase in Thermal Lag Due To Addition of Insulation

Walls Without Insulation			Walls with Insulation				Increase in M	Increase in Thermal Lag, h
Designation	M	Thermal Lag, h	Designation	M	Thermal Lag, h	Insulation		
M1	0.68	3.0	M2	0.91	3.5	Expanded perlite in block core	0.23	0.5
M3	0.85	4.5	M4	1.11	6	Expanded perlite in cavity	0.26	1.5
M9	0.91	5.5	M10	1.21	7	Expanded perlite in cavity	0.30	1.5
C1	0.76	4.0	C4	0.83	5	Polyisocyanurate on outside surface	0.07	1.0

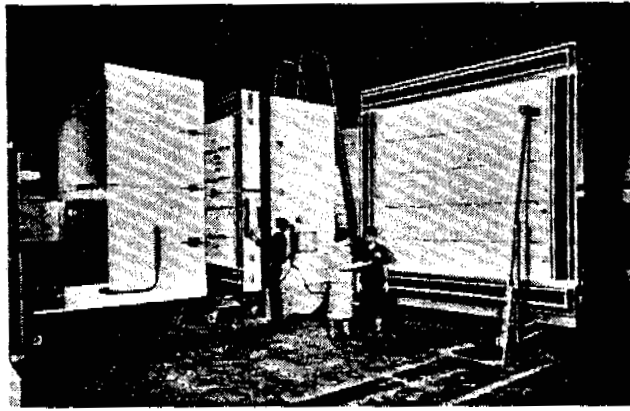


Figure 1. Calibrated hot box test facility

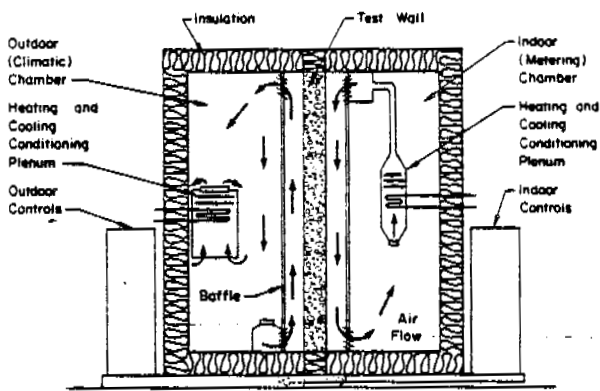


Figure 2. Schematic of calibrated hot box

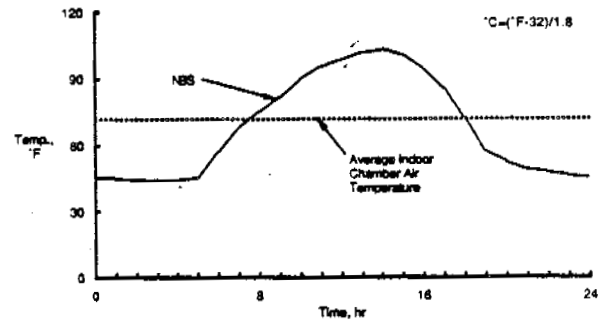


Figure 3. Outdoor chamber-air temperature for NBS dynamic test cycle

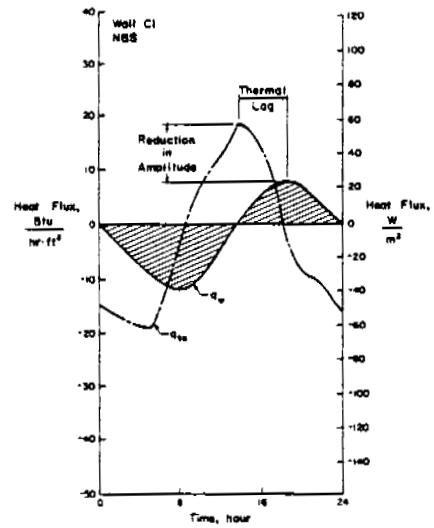
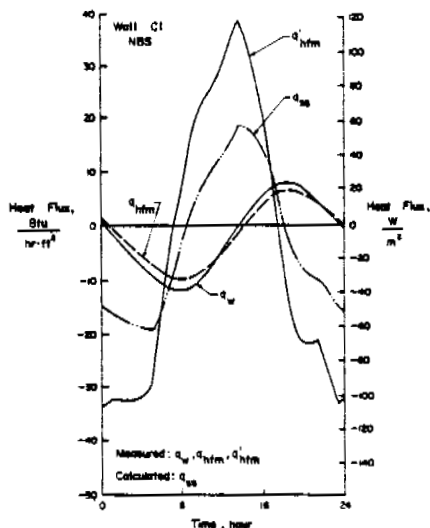


Figure 4. Dynamic test results for NBS temperature cycle applied to wall C1 (normal weight concrete): measured and calculated heat flux (left) and definitions of dynamic heat transmission coefficients (right)

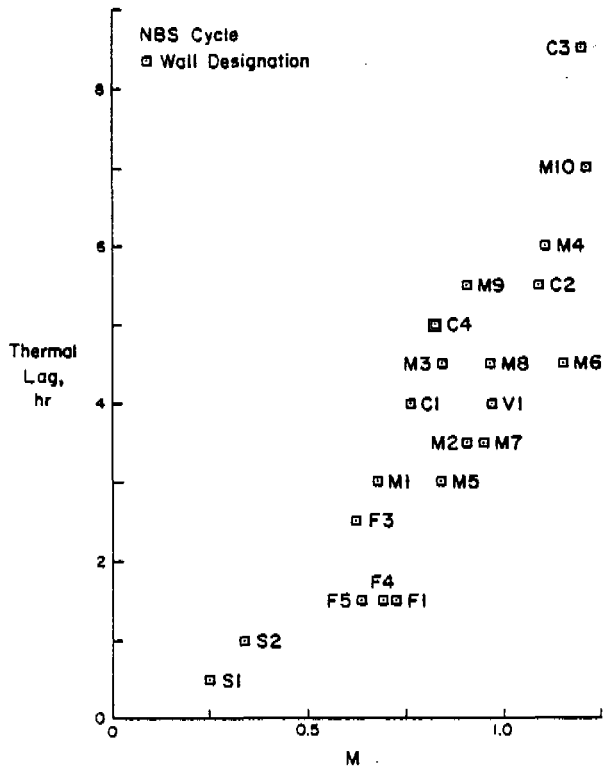


Figure 5. Thermal lag and M values for the NBS test cycle applied to 21 wall assemblies

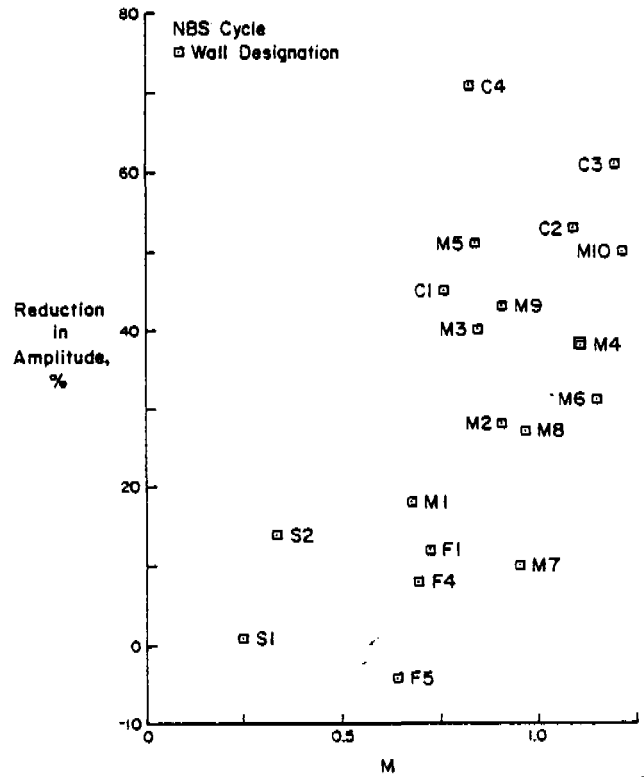


Figure 6. Reduction in amplitude and M values for the NBS test cycle applied to 19 wall assemblies

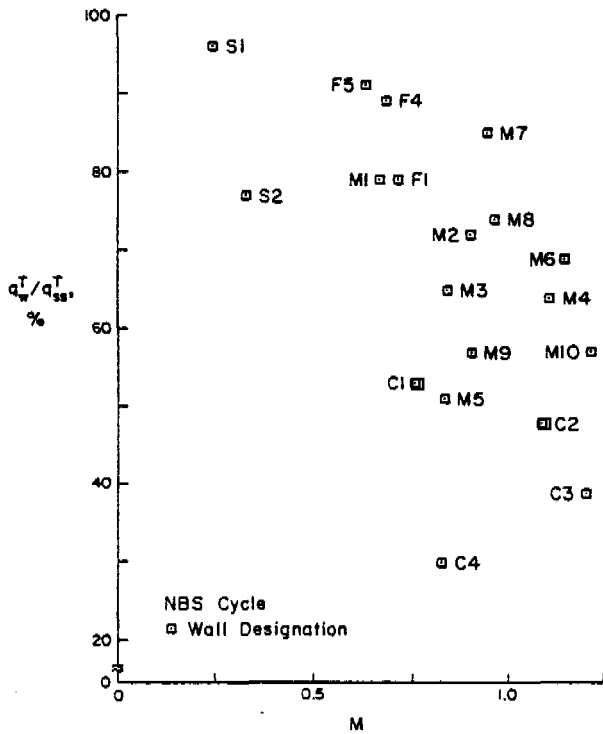


Figure 7. Total heat flow ratios and M values for the NBS test cycle applied to 19 wall assemblies

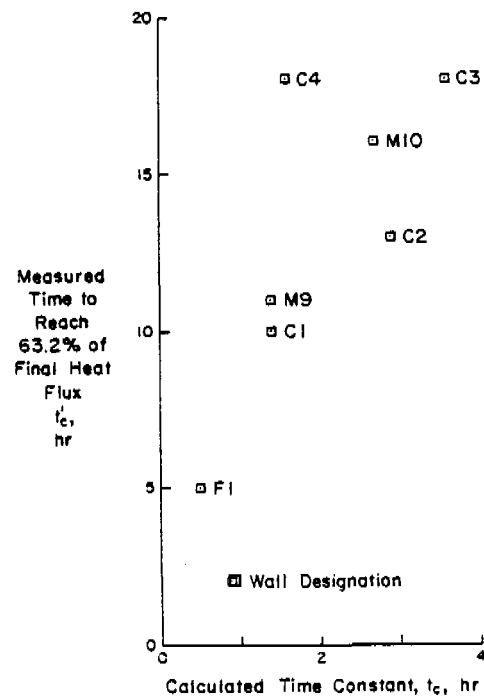


Figure 8. Transient test results compared to calculated time constants